Baseline design of laser fusion research reactor with MW class laser facility

PAPER • OPEN ACCESS

Baseline design of laser fusion research reactor with MW class laser facility

To cite this article: Akifumi Iwamoto *et al* 2024 *Nucl. Fusion* **64** 086068

OPEN ACCESS
IOP Publishing | International Atomic Energy Agency
Nuclear Fusion
Nucl. Fusion **64** (2024) 086068 (12pp)
https://doi.org/10.1088/1741-4326/ad573d

Baseline design of laser fusion research reactor with MW class laser facility

Akifumi Iwamoto[1,*], Masahiro Tanaka[1], Keisuke Shigemori[2] and Ryosuke Kodama[2]

[1] National Institute for Fusion Science, Oroshi/Toki, Japan
[2] Institute of Laser Engineering, Osaka University, Yamadaoka/Suita, Japan

E-mail: iwamoto.akifumi@nifs.ac.jp

Received 15 January 2024, revised 8 May 2024
Accepted for publication 12 June 2024
Published 15 July 2024

Abstract

We propose a sub-ignition/burning reactor which is named the Laser-fusion Subcritical Power Reactor Engineering Method (L-Supreme). The reliabilities of L-Supreme in a MW class laser facility are assessed with respect to the following points: a reactor core, a target chamber, a target delivery system, an Exhaust Detritiation System (EDS), and neutron shielding. The Japan Establishment for Power-laser Community Harvest (J-EPoCH) would be applied as a MW class laser facility. A non-cryogenic glass balloon target filled with gaseous deuterium-tritium (DT) is contained in a target capsule. A chain-type magazine system might be used for a mass supply of the target capsules. Each target capsule is delivered to the center of a reactor core at 1 Hz. A batch of 10 000 laser shots would realize 0.22 MJ fusion power. The amount of tritium per batch is 1.51×10^{12} Bq. During laser experiments, unburned tritium is evacuated and transferred into an Exhaust Detritiation System (EDS). An evacuation rate of more than 0.1 m^3 s^{-1} is required in order to recover less than 5000 Bq m^{-3} of the threshold of tritium concentration within 1 h. For safety, emergency situations such as tritium leakage in facilities are examined. The EDS works by internal circulation processes. Assuming leakage of tritium for a batch, an air circulation flow rate of 4100 Nm^3 h^{-1} is required in an experimental hall for recovering less than 5000 Bq m^{-3} within 48 h. A primary and secondary neutron shield concept are proposed and would provide full neutron shielding. We conclude that it is possible to construct the L-Supreme system by marshalling current technologies.

Keywords: laser fusion, research reactor, baseline design, replaceable core, EDS, neutron shielding, J-EPoCH

(Some figures may appear in colour only in the online journal)

1. Introduction

In recent years, fusion research into burning plasma has progressed. For instance, DT burning at ITER is planned in 2035 [1], and the National Ignition facility (NIF) is achieving laser-driven inertial fusion, so called laser fusion, ignition and burning using Deuterium-Tritium (DT) fuel [2, 3]. Fusion research advances the development of fusion reactors, and DEMO ones have been designed for fusion energy demonstration. Furthermore, several types of fusion reactors have been proposed from nuclear fusion startups such as Commonwealth Fusion Systems (CFS), Helion, and General Fusion, in order to realize fusion energy. However, the startups have not described the strategy of converting fusion energy into thermal or electrical energy. Thus, the most important element of fusion reactors is left undefined. Strategies only for DEMO reactors

* Author to whom any correspondence should be addressed.

have been presented. Test blanket modules are designed for investigation, using ITER burning plasma, no earlier than 2035 [4]. Limited blanket space within magnets is available for magnetic confinement fusion.

In the United States of America (USA), discussion about development of inertial fusion energy started from the NIF achievement [5]. Laser fusion is the mainstream of inertial fusion and its development plan should be different from strategies for DEMO reactors. This is because of a substantial difference in a DT fusion source between magnetic confinement and laser fusion [6]. The point DT fusion source of laser fusion omnidirectionally releases alpha particles and neutrons. The effects on laser fusion reactors by alpha particles must be more severe than those on magnetic confinement fusion reactors [7]. However, laser fusion has a high flexibility of blanket design and in principle, blanket space is not limited. The distance from the point fusion source controls the fluxes of alpha particles and neutrons. In terms of the blanket system, laser fusion has an advantage.

Several fundamental blanket technologies such as tritium breeding, n-t conversion and so on, are common to both magnetic confinement and laser fusion reactors. However, the requirements of each reactor system for the fusion burning method, blanket, fueling, coolants, etc, depend on reactor designs [8, 9]. For example, the limited blanket space of magnetic confinement fusion demands lithium isotope enrichment, in order to breed tritium fuel [10, 11]. Fusion reactor engineering research dedicated to laser fusion reactors should be initiated.

In order to realize inertial fusion energy, laser fusion engineering research should be conducted in parallel with laser plasma physics research. However, to date, facilities for laser fusion research have been dedicated to physics research, unlike magnetic confinement fusion study [12, 13]. Therefore, facilities for laser fusion engineering research are required. The facilities should have the functions of laser fusion reactors [8, 14–16], such as repetition of laser shots, energy conversions and tritium breeding. Studies on several components: high repetition lasers [17, 18], target injection [19–21], target engagement [22–26], a mass production of targets [27–29] have already been initiated. Existing technologies can realize a laser fusion research reactor utilizing sub-ignition/burning fusion reactions. Therefore the Laser-fusion Subcritical Power Reactor Engineering Method (L-Supreme) with a MW class laser facility has been proposed for laser fusion engineering research. Regarding the reactor name, the word 'subcritical' means the condition before ignition. In the conceptual design, the possibilities of reactor cores were estimated as follows. L-Supreme would become a DT fusion neutron source for studying fusion engineering issues: neutron-thermal and thermal-electrical energy conversions, tritium breeding and irradiation effects of materials. Furthermore, power generation of a few watts would be demonstrated, using a dedicated core, as discussed in [30]. It is expected that integration of 10 000 shots generates ∼0.22 MJ of thermal fusion power. However, the feasibility of L-Supreme as a laser fusion research reactor system has not been assessed. Therefore, the specifications of the whole system are discussed, and the baseline design as a laser fusion research reactor system is set out.

2. Conceptual design of L-Supreme in the previous studies

A multi-purpose high repetition laser facility, the so-called Japan Establishment for Power-laser Community Harvest (J-EPoCH) is proposed as a next generation laser facility [30]. J-EPoCH will operate at a maximum rate of 100 Hz. A high-performance laser with high average power of 1 kW and a high repetition rate of 100 Hz has been developed as a module laser technology for J-EPoCH [17]. As one of the applications of J-EPoCH, L-Supreme has been conceptually designed based on existing technologies [30, 31]. Twelve omnidirectional laser beams with 8 kJ would yield $\sim 10^{13}$ neutrons using a Large diameter High Aspect Ratio Target (LHART) [32, 33]. The conceptual design is focused on the capabilities of reactor cores. In the design study, the effects of the core size were considered regarding n-t conversion and tritium breeding by the Particle and Heavy Ion Transport code System (PHITS) version 3.20 calculations [34]. A thermal fusion power of 21.4 W will be generated in a $Li_{17}Pb_{83}$ core with an 80 cm thickness at 1 Hz operation. The $Li_{17}Pb_{83}$ core with 100 cm thickness can yield more than one tritium from a DT fusion neutron. Opportunities of neutron irradiation with a fluence of $\sim 6.6 \times 10^{13}$ n m^{-2} per shot (a neutron flux of 6.6×10^{13} n m^{-2} s^{-1} at 1 Hz operation) will be also provided at a radius of 10 cm. Ten years operation at 1 Hz results in a neutron fluence of 2.1×10^{22} n m^{-2} at the inner surface of the core. However, high neutron flux irradiation effects on blanket materials for fusion power demonstration plant (DEMO) designs cannot be examined because the neutron flux in L-Supreme is several orders of magnitude lower than that at the DEMO blanket system [35, 36]. The conceptual design shows us the ability of L-Supreme to conduct fusion engineering research.

3. Baseline design of L-Supreme

L-Supreme consists principally of four systems: a core, a target chamber, a target delivery system, and an Exhaust Detritiation System (EDS), except in J-EPoCH. As this design, the whole system of L-Supreme is discussed, and its feasibility is assessed. A bird's-eye view of L-Supreme is shown in figure 1. The specification of each system is described below.

3.1. Reactor core

DT fusion reactions release alpha particles and neutrons. Neutrons are a main energy source, and therefore, conventional blanket design focuses on the energy conversion from neutrons. A core is a hollow sphere with a core material thickness up to ∼1 m which is sandwiched between a neutron multiplier and reflector materials, as shown in figure 2. For fusion engineering research, a core is replaceable by others, and we should prepare several core materials including graphite, Li, and $Li_{17}Pb_{83}$, which are planned for use in future experimental

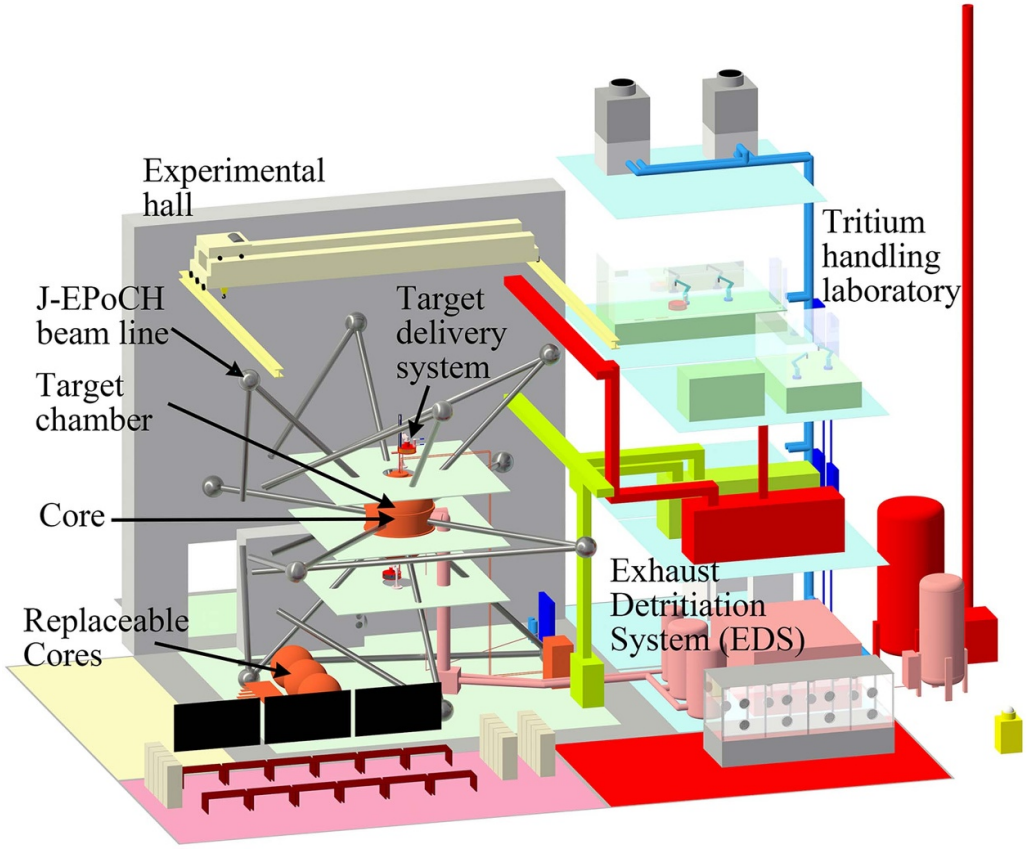

Figure 1. Bird's-eye view of L-Supreme.

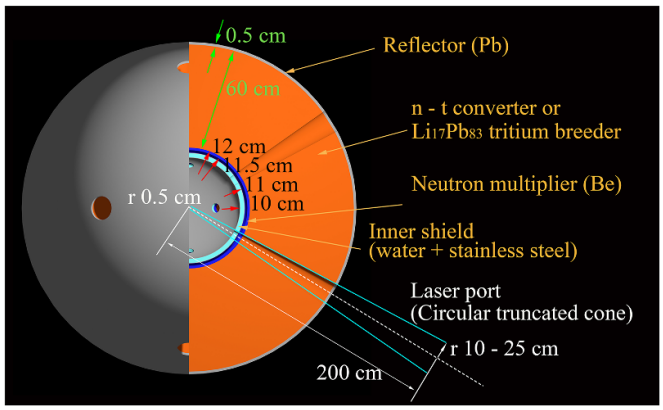

Figure 2. Core model [31]. Reproduced from [31].© 2021 IAEA, Vienna. All rights reserved.

reactors. The capabilities of the cores have been reported in [31].

In terms of laser fusion reactors, omnidirectionally released alpha particles are essential. According to PHITS calculations, alpha particles are stopped at the inner surface of the cooling water sphere, as shown in figure 3, which might result in radiation degradation of the surface. Laser ports allow alpha particles to be transmitted out of the core. The inner surface faces the DT fusion source at a 10 cm distance. An alpha energy of 44.6 J m^{-2} per shot would be formed at the inner surface, and a fluence of alpha particles of 7.96×10^{13} m^{-2} per shot is expected. The effects of the alpha particles on the surface should be negligible in the case of L-Supreme. For commercial laser fusion reactors, neutrons moderately give their energy to core materials while penetrating a reactor core; however, the energy of alpha particles is yielded in the vicinity of the surface of reactor components. Therefore, the high flux irradiation of the alpha particles might be problem. The impact of the alpha particles should be adjusted by their distance from DT reactions.

To date, several types of neutron-free fusion reactors has been proposed for generating fusion reactions: 11B(p, 3α) and 3He(d, p)4He. The energy of protons is also yielded in the vicinity of the surface of reactor components. Technically, reactor designs using pB11 and DHe3 fusion reactions cannot adopt a conventional blanket system. Energy conversion technologies from the fusion reactions to thermal or electrical energy are still remaining issues. Suitable methods of energy conversion for each fusion reaction need to be proposed. An adjustable core size of L-Supreme is relevant to research into power generation from alpha particles.

3.2. Target fabrication and delivery

The technology of the LHART has been established which uses a glass balloon with a 1 mm diameter. Gaseous DT permeates and fills the glass balloon at a high temperature.

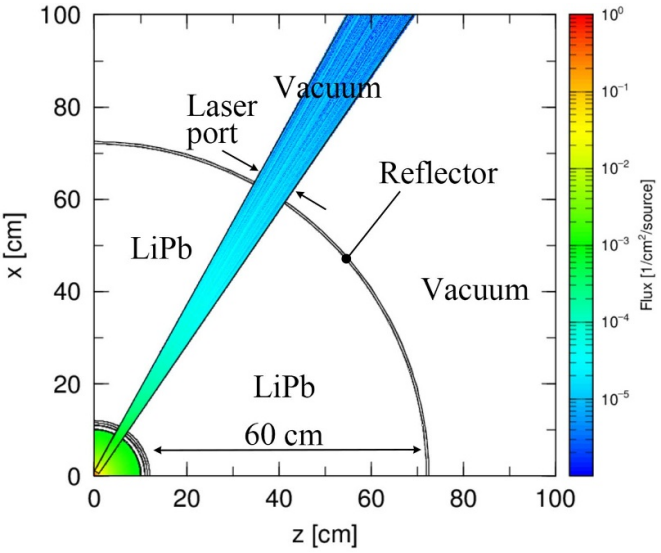

Figure 3. Fluence of alpha particles. Core with LiPb layer of 60 cm in thickness and $r = 10$ cm laser port.

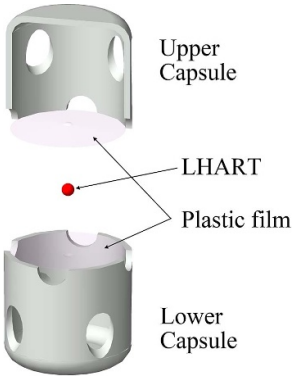

Figure 4. LHART in a target capsule.

Thus the LHART contains gaseous deuterium-tritium (DT) at ∼600 kPa, which corresponds to tritium of 1.51×10^8 Bq, and is set in a capsule for easy handling, as shown in figure 4. The permeation and capsuling processes are completed in a glove box. The capsules are delivered to the center of the core one by one with ∼10 μm precision at 1 Hz, using a mechanical target delivery system. Linear motors are a candidate for a drive mechanism. Speed and acceleration of linear motors exceed 14 m s^{-1} and 1600 m s^{-2}, respectively [37]. It might take several 100 ms to complete a reciprocating motion of a target delivery. A target delivery rate is limited by a linear motor drive. Ten-thousand targets are planned to be used in a batch of laser shots. A chain-type magazine system might be used for a mass supply of target capsules, as shown in figure 5. For L-Supreme, the capsules should be reused because a low fusion output of 22.4 J/shot would not damage the capsules.

The target capsule might work as a radiation shielding. A cylinder capsule with a 10 mm outer radius and 35 mm height is assumed and is made of 5083 aluminum alloy, 1 mm thick. Shielding effects of the capsule without laser penetrations are calculated by the PHITS. Figure 6 shows fluences of neutrons and alpha particles through the capsule. A neutron fluence drop is negligible at the capsule wall. On the other hand, the target capsule fully shields alpha particles. Therefore capsule designs should be considered to meet experimental requirements.

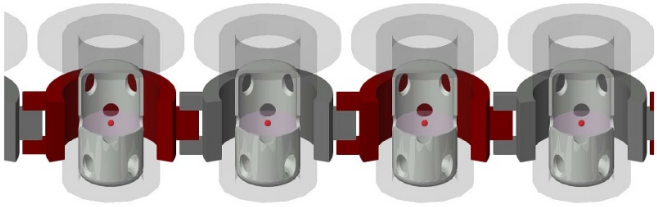

Figure 5. Image of chain type magazine.

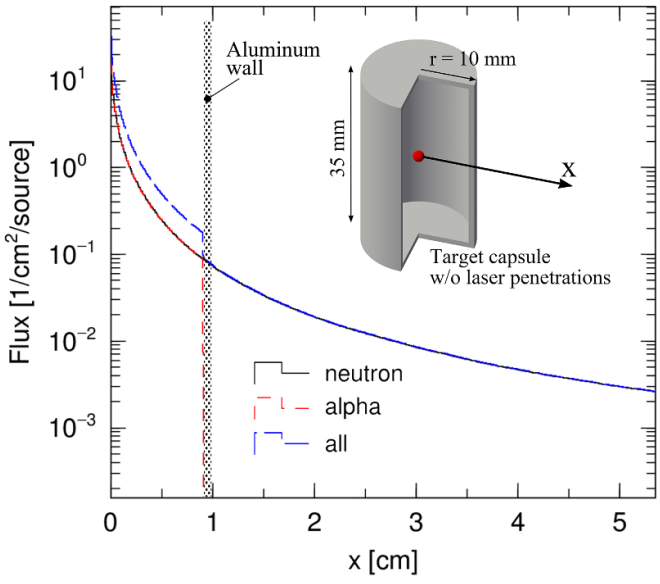

Figure 6. Fluences of neutrons and alpha particles through the target capsule.

3.3. *Target chamber*

In the present design, the target chamber is spherical and its diameter is 3.0 m. The chamber includes ports for laser beams, core replacement, vacuum pumps, plasma diagnostics, and the target delivery system. Stainless steel is selected as the chamber material because of easy fabrication with high precision. Aluminum alloys can be one of candidate materials to minimize radioactivation, because the chamber does not work as a structural support for heavy items [38]. According to the Japan Industrial Standard (JIS) B8267 2020 [39], the required thicknesses of the target chamber walls made from 316L stainless steel and 5083 aluminum alloy [38] are estimated. The outside and inside pressures of the chamber are assumed to be 0.15 MPa and 1.33×10^{-3} Pa, respectively. For these estimations, a target chamber without any ports is assumed. Thicknesses of 6 mm and 10 mm are required for the chamber walls made from 316L stainless steel and 5083 aluminum alloy, respectively. Ports inevitably increase the required thickness of the chamber wall. Mechanical analyses

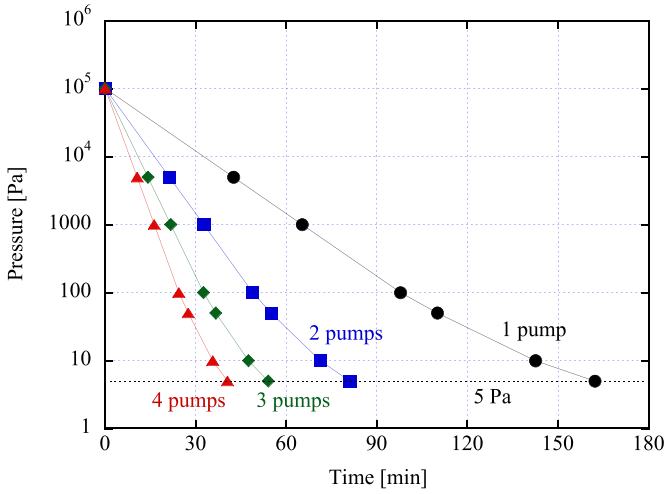

Figure 7. Evacuation curves of the target chamber with ISP-1000E.

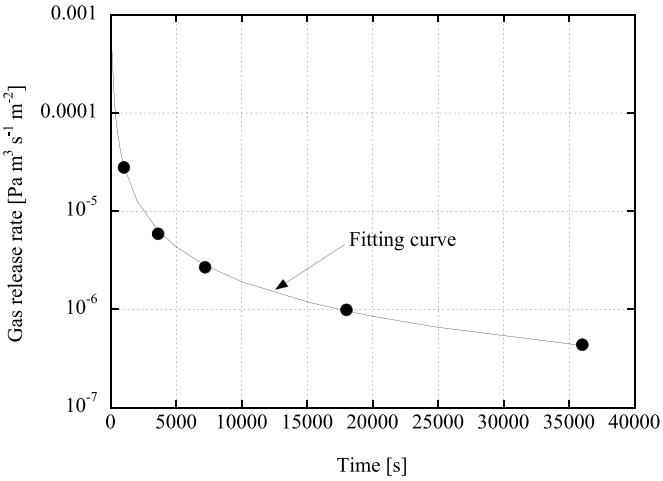

Figure 8. Outgassing rate from GBB stainless steel surface from [41]. Reprinted from [41], Copyright (1996), with permission from Elsevier.

will be conducted after the assignment of ports, in order to complete the engineering design of the chamber.

The performance of a vacuum pump system is considered from evacuation time. In this design, an hour is assigned for the evacuation time, and the target pressure is 1.33×10^{-3} Pa. The system is assumed to consist of turbomolecular and dry scroll vacuum pumps. For the evacuation time estimation, an example of a dry scroll vacuum pump: ISP-1000E (Anest Iwata Corporation) is given [40]. The pumping speed of ISP-1000E depends on the chamber pressure and is 1000 l min^{-1} around atmospheric pressure. The scroll pump governs atmospheric pressure to 5 Pa. The evacuation time is calculated using the following equation

$$t = \frac{V}{S} \ln \frac{p_0}{p} \tag{1}$$

t: evacuation time
V: chamber volume
S: pumping speed
p_0: initial pressure
p: ultimate pressure.

Figure 7 represents the evacuation curve of the target chamber (14.14 m^3). More than four pumps are required in order to meet the design specifications.

Turbo molecular pumps governs a pressure range from 5 Pa to 1.33×10^{-3} Pa. The evacuation time is calculated using the following equation

$$V\frac{\mathrm{d}p}{\mathrm{d}t} = -S\left[p\left(t\right) - p_u\right] + Q \tag{2}$$

V: Chamber volume (m^3)
$p(t)$: pressure (Pa)
p_u: Ultimate pressure of turbo molecular pump (Pa)
S: Pumping speed (l s^{-1})
Q: Outgassing rate from surfaces (Pa m^3/s m^2).

As an outgassing rate from the chamber surface, the data on a surface finished by glass bead blasting (GBB) was indicated

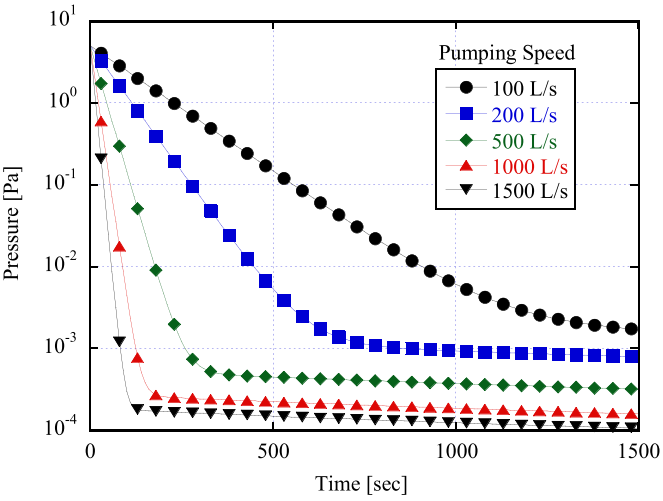

Figure 9. Dependence of evacuation curves on pumping speeds of turbomolecular pumps.

[41]. Figure 8 represents the outgassing rate from the GBB surface. After the target shots, a tritium release rate should be considered. In terms of laser fusion experiments, the estimation of the tritium release rate from target chamber surfaces has not been reported. Therefore, we refer to an estimation from magnetic fusion experiments. According to data from LHD experiments, a tritium release rate of 8.8×10^{-12} Pa m^3 s^{-1} m^{-2} from the vacuum vessel has been evaluated [42]. The tritium releasing rate is negligibly small compared with the outgassing rate from the GBB stainless steel surface. Figure 9 shows the dependence of evacuation curves on pumping speeds. Higher pumping speeds can achieve both lower pressure and a short evacuation time. In order to achieve a 1 h evacuation time, a pumping speed of more than 500 l s^{-1} is required. Outgassing and tritium release rates strongly depend on experimental history, and therefore should be evaluated under laser fusion reactor conditions.

The target chamber works as a tritium boundary in regular experiments. Unburned DT is left in the target chamber. Connecting vacuum pumps evacuate gaseous DT from the chamber. The gaseous DT is transferred to the EDS. Different core materials should be prepared depending on research purposes. When a core is replaced by another, the target chamber is opened to the experimental hall. It might result in release of a trace of tritium. The EDS must make the resulting tritium concentration low.

3.4. EDS

An EDS applying conventional technologies will be installed to ensure safe tritium handling and is equipped with two operation modes: 'normal' and 'emergency'. A high-level system and three low-level ones are planned. In the normal mode, the high-level system works for laser fusion experiments. Tritium of 1.51×10^8 Bq is contained in the LHART. During a batch of 10 000 laser shots, tritium of 1.51×10^{12} Bq is released in the target chamber. The tritium is evacuated by a vacuum pumping system and flows to the EDS. Low-level systems work for the target chamber, the experimental hall, the glove box, and the tritium handling laboratory.

From Laws Concerning the Prevention of Radiation Hazards due to Radioisotopes and Others in Japan, regulations on the tritium concentration of water vapor and gas state that, for the public, they must be lower than 5000 Bq m^{-3} and 7.0×10^7 Bq m^{-3}, respectively. For radiation workers, a tritium concentration up to 8.0×10^5 Bq m^{-3} of water vapor and 1.0×10^{10} Bq m^{-3} of gas are allowable. In this design, 5000 Bq m^{-3} of tritium concentration is assigned as the threshold for both water vapor and gas.

3.4.1. Normal operation. For normal operations, the EDS works by once-through processes. In this mode exhausted tritium is oxidized and recovered as tritiated water, which is then sent to storage tanks. The ability of the EDS with once-through processes is estimated using the following equation

$$V\frac{\mathrm{d}c}{\mathrm{d}t} = -Q\left[c\left(t\right) - c_0\right] + M \tag{3}$$

V: Volume of a chamber, a glove box and rooms (m^3)
$c(t)$: Tritium concentration in the volume (Bq m^{-3})
c_o: Tritium concentration in outside air (Bq m^{-3})
Q: Purge flow rate or pumping speed ($Nm^3\ h^{-1}$) or ($m^3\ s^{-1}$)
M: Tritium release rate from surfaces (Bq h^{-1}) or (Bq s^{-1}).

During laser experiments, tritium is released only in the target chamber. One Hz target shots result in a tritium release rate of 1.51×10^8 Bq s^{-1}. In the equation (3), the tritium release rate of 1.51×10^8 Bq s^{-1} is assigned as M. The tritium concentration in the outside air should be 0 Bq m^{-3}. Figure 10 shows the dependence of tritium concentration in the chamber on evacuation rates in a range of 0.2–5.0 $m^3\ s^{-1}$. After starting a laser experiment, the tritium concentration in the chamber quickly increases and then reaches a constant value. The lower evacuation rate makes the tritium concentration higher.

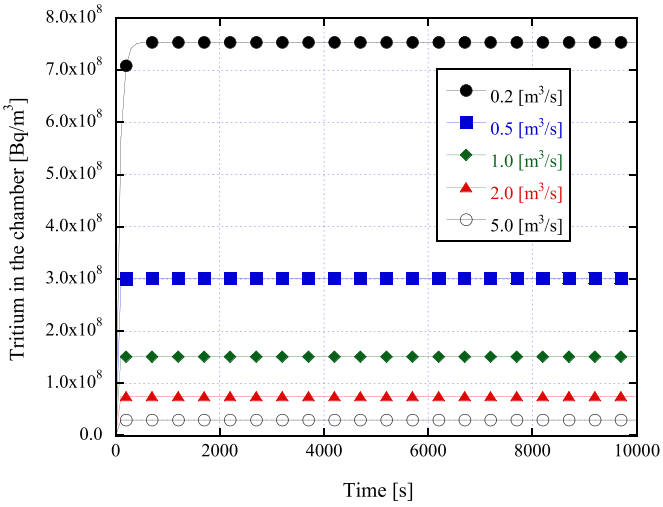

Figure 10. Dependence of tritium concentration in the chamber on evacuation rates.

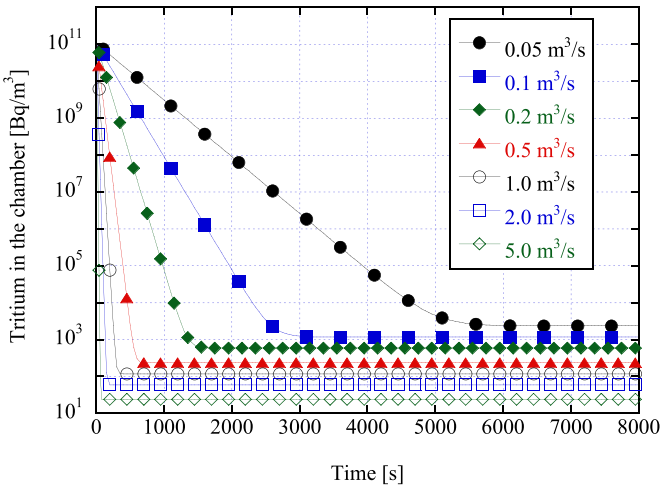

Figure 11. Dependence of tritium concentration in the chamber after 10 000 target shots on evacuation rates.

After a batch of 10 000 laser shots, tritium of 1.51×10^{12} Bq, which corresponds to 1.07×10^{11} Bq m^{-3}, remains in the target chamber at the maximum. The tritium removal ability of vacuum pumps is calculated in an evacuation rate range of 0.05−5.0 $m^3\ s^{-1}$. Referring to the estimation from the Large Helical device, a tritium release rate and a tritium concentration in the outside air can be assumed to be 4.17 Bq m^{-2} s [42] and 0.05 Bq m^{-3} [43], respectively. Figure 11 shows the achieved tritium level after the evacuation. The tritium concentration must be lower than 5000 Bq m^{-3}. Evacuation rates of more than 0.1 $m^3\ s^{-1}$ can achieve less than 5000 Bq m^{-3} within 1 h. Then the target chamber can be opened.

During maintenance after opening the chamber, the tritium concentration in the target chamber should be kept at less than 5000 Bq m^{-3}. To calculate the tritium concentration in the chamber, it starts from 5000 Bq m^{-3}. A tritium release rate from the chamber surface and a tritium concentration in the

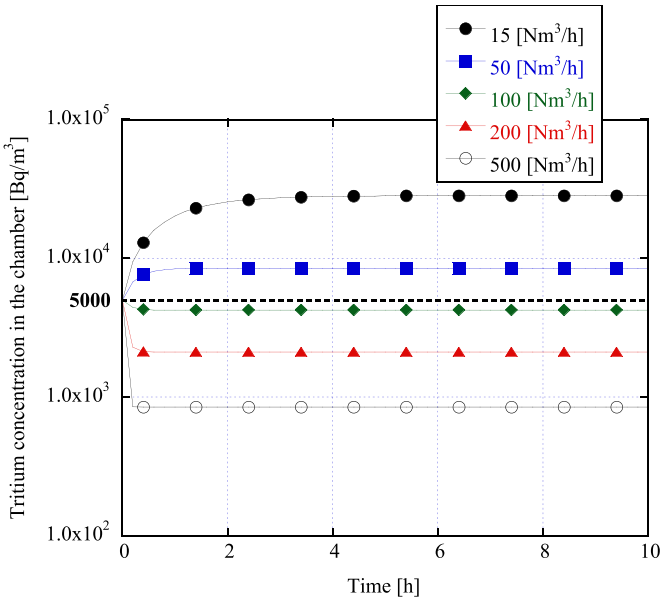

Figure 12. Dependence of tritium concentration achievement in the chamber on purge flow rates.

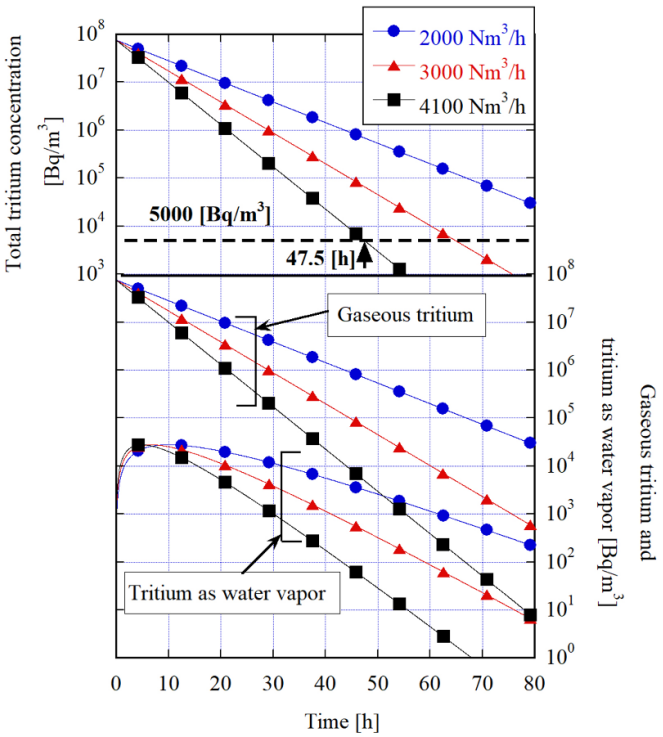

Figure 13. Dependence of tritium concentration achievement in the experimental hall on purge flow rates.

outside air are assumed to be 4.17 Bq m^{-2} s and 0.05 Bq m^{-3}, respectively, as mentioned above. Figure 12 shows the dependence of tritium concentration in the chamber on purge flow rates, and one of more than 100 Nm^3 h^{-1} is required to be kept at less than 5000 Bq m^{-3}.

Required purge flow rates of the experimental hall, the tritium handling laboratory, and the EDS room should be considered. However, there is no information on the tritium release rate from surfaces of buildings. Therefore, the building standard law derived from ventilation of persons is taken into account. Assuming the maximum number of persons in their rooms, purge flow rates of the experimental hall, the tritium handling laboratory, and the EDS room are set at 3400 Nm^3 h^{-1}, 400 Nm^3 h^{-1}, and 500 Nm^3 h^{-1}, respectively, as tentative specifications.

3.4.2. Emergency operation. For an emergency situation such as tritium leakage, the EDS works by internal circulation processes. Tritium leakage might occur in the experimental hall, the tritium handling laboratory and the EDS room. In this mode, a part of the tritiated water would return with circulating air because the EDS processes do not reach 100% efficiency of tritium recovery. The ability of the EDS in the circulation mode is estimated using the following equations

$$V\frac{\mathrm{d}c_{\mathrm{T_2}}}{\mathrm{d}t} = -Fc_{\mathrm{T_2}} + \alpha Fc_{\mathrm{T_2}} \tag{4}$$

$$V\frac{\mathrm{d}c_{\mathrm{T_2O}}}{\mathrm{d}t} = -Fc_{\mathrm{T_2O}} + \beta Fc_{\mathrm{T_2O}} + (1-\alpha)F\cdot\beta c_{\mathrm{T_2}} \tag{5}$$

$$c_{\mathrm{T_2}}(t) + c_{\mathrm{T_2O}}(t) = c(t) \tag{6}$$

$c_{\mathrm{T_2}}(t)$: Gaseous tritium concentration in the volume (Bq m^{-3})

$c_{\mathrm{T_2O}}(t)$: Tritiated water concentration in the volume (Bq m^{-3})

F: Circulation flow rate (m^3 h^{-1})

1-α: Conversion rate of tritium to tritiated water

1-β: Removal rate of tritiated water.

The worst case of releasing 1.51 $\times$ 10^{12} Bq tritium is assumed. The EDS is designed so that the experimental hall and other places can recover within 48 h and 12 h, respectively. The tritium concentration should be lowered to less than 5000 Bq m^{-3}. It is assumed that there is no tritiated water in the experimental hall at the beginning and that tritium is released as hydrogen. A conversion rate of tritium to tritiated water and a removal rate of tritiated water are assumed to be 0.990 [44] and 0.999% [45], respectively, from past achievements. Figure 13 shows trends of tritium concentration on circulation flow rates: 2000, 3000, and 4100 Nm^3 h^{-1} in an experimental hall of 20 000 m^3. After starting air circulation, the concentration of tritium water vapor quickly increases because circulating air contains tritiated water unrecovered in the EDS. However, the total tritium concentration is little affected by the small concentration of the tritiated water vapor. A flow rate of 4100 Nm^3 h^{-1} is required for recovering a tritium concentration of less than 5000 Bq m^{-3} within 48 h. This processing capability is comparable to that of the ITER tritium plant [46]. Trends of tritium concentration on circulation flow rates: 300, 400, 500, and 600 Nm^3 h^{-1} in a tritium handling laboratory of 400 m^3 are also calculated, as shown in figure 14. A circulation flow rate of 500 Nm^3 h^{-1} is required for recovering a tritium concentration of less than 5000 Bq m^{-3} within 12 h. For an EDS room of 2000 m^3, a required circulation flow

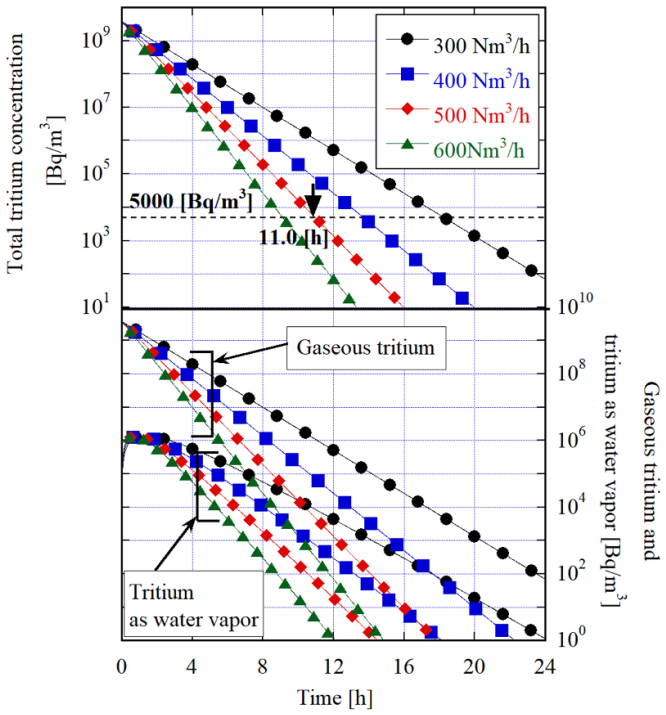

Figure 14. Dependence of tritium concentration achievement in the tritium handling laboratory on purge flow rates.

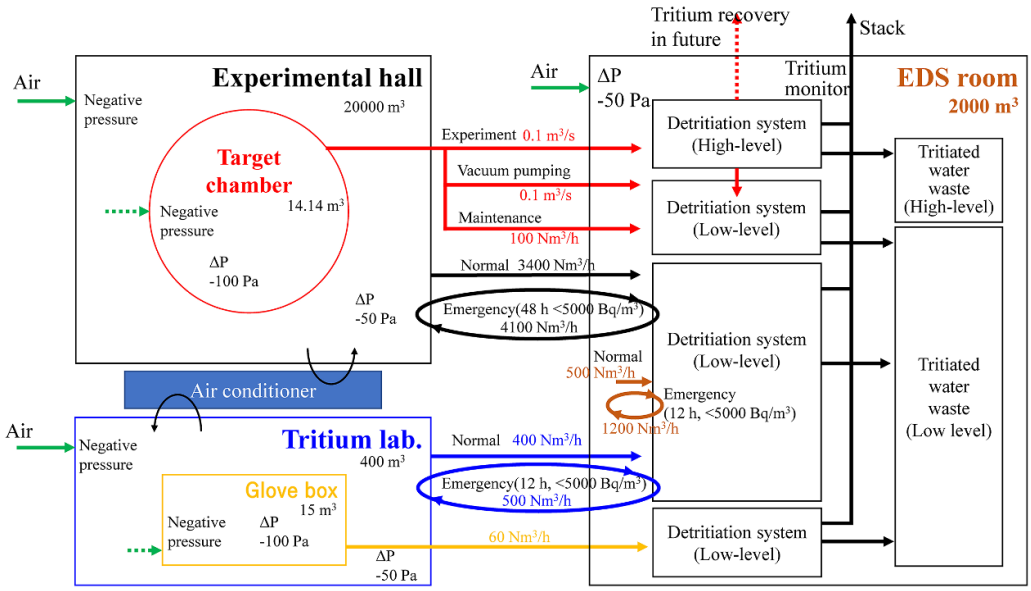

Figure 15. Flow diagram of EDS for L-Supreme.

rate is estimated in the same manner. A circulation flow rate of 1200 Nm^3 h^{-1} can decrease the tritium concentration to less than 5000 Bq m^{-3} within 12 h.

According to the calculations above, specifications of the EDS are summarized. In terms of the target chamber, pumping speeds of 0.5 m^3 s^{-1} and 0.1 m^3 s^{-1} are required after maintenance and a batch of laser experiments, respectively, as required of turbomolecular pumps. During maintenance, a purge flow rate of more than 100 Nm^3 h^{-1} can achieve less than 5000 Bq m^{-3} of the tritium concentration in the chamber. Purge flow rates of the experimental hall, the tritium handling laboratory, and the EDS room are tentatively assigned at 3400 Nm^3 h^{-1}, 400 Nm^3 h^{-1}, and 500 Nm^3 h^{-1}, respectively, in normal operations. After a tritium leakage event, the EDS works in the emergency mode. Circulation flow rates of 4100 Nm^3 h^{-1}, 500 Nm^3 h^{-1}, and 1200 Nm^3 h^{-1} for the experimental hall, the tritium handling laboratory, and the EDS room, respectively, are required. Figure 15 shows the flow diagram of the EDS for L-Supreme.

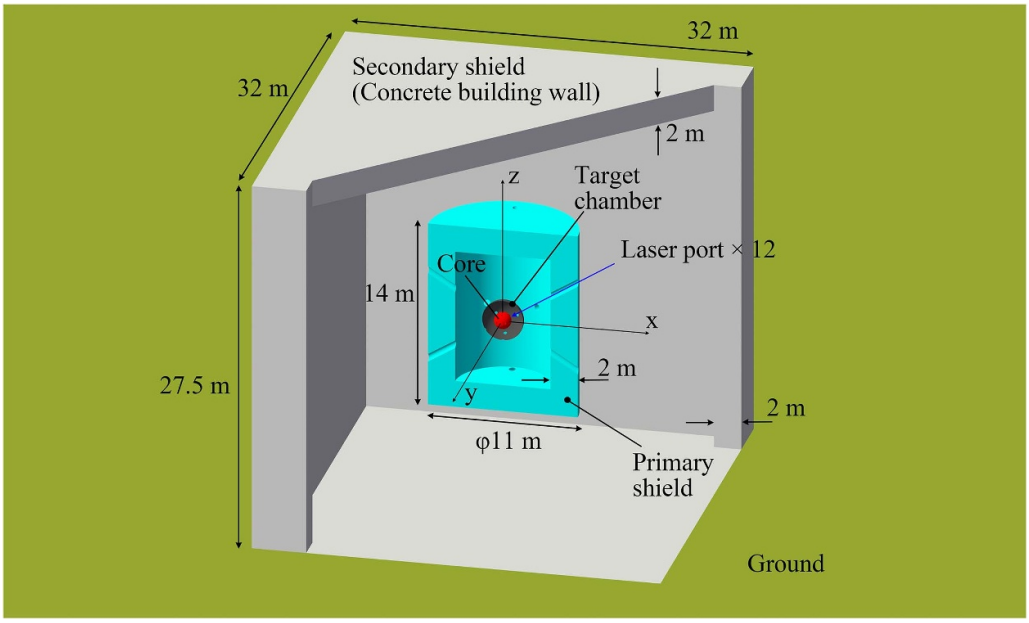

Figure 16. Model for neutron and alpha energy deposited.

Table 1. Composition of concrete. Reproduced with permission from [48]. Copyright © Atomic Energy Society of Japan. All rights reserved.

Concrete	H	O	Na	Mg	Al	Si	S	K	Ca	Ti	Fe
2.200	0.010	1.061	0.041	0.019	0.128	0.646	0.002	0.057	0.171	0.009	0.055

(g cm^{-3}).

4. Neutron shielding

Neutron shielding must be considered in order to secure the safety of fusion reactors. A reactor core for laser fusion reactors will have penetrations such as laser ports, target injection, target tracking, vacuum systems, maintenance access, etc. Neutrons from DT fusion reactions can leave a reactor core through the penetrations. The target chamber does not provide neutron shielding not only because of the penetrations, but also there is little shielding effect from the target chamber materials. Concrete is a conventional shielding material and has been used as such in the NIF [47]. Single shot yields of up to 1.6×10^{19} neutrons are assumed for the NIF facility design. The 2 m primary and 1 m secondary shielding walls provide full protection. A primary and secondary shield concept is intended to be used in the L-Supreme design. The primary shielding consists of a cylindrical concrete wall with laser apertures, which reduces neutron flux. Then the secondary shielding prevents neutrons from reaching outside the reactor building. Yields of 10^{17} neutrons from 10 000 shots are expected in our batch experiment. More than a two order difference between the NIF and L-Supreme might allow us to design a lower-cost shielding system.

4.1. Model of shielding system

The model consists of a core with 12 laser ports, a spherical target chamber with 12 laser ports, primary concrete shielding with 12 laser apertures, and secondary shielding of concrete walls, as shown in figure 16. A graphite core, 1 m thick, is used in the model, and the composition of the core is described in chapter 3.1. A spherical target chamber with a 1.5 m inner radius is assumed and is made of 304 stainless steel, 2 cm thick. A cylindrical primary concrete wall, 2 m thick, surrounds the target chamber. The wall of the experimental hall, 2 m thick, provides the secondary shield. The model excludes J-EPoCH. However, an adjoining laser hall should be continuous secondary shielding. The composition of shielding concrete used in a nuclear reactor in Japan, is referred as listed in table 1 [48].

4.2. Energy deposited in experimental hall

Energy deposited from a DT fusion reaction is calculated by the PHITS. The experimental hall with and without primary shielding is compared. Figures 17 and 18 show profiles of energy deposited on the *x*-*y* plan. Most of the neutrons are stopped at the concrete wall of the primary shielding. Remaining neutrons are transmitted to the experimental hall through laser ports and then scattered in all directions. No primary shielding increases the absorbed dose in the experimental hall as shown in figure 18. The primary shielding is effective in reducing the energy deposited in the experimental hall. The concrete wall, 2 m thick, prevents neutrons from reaching the surrounding area of the experimental hall. The

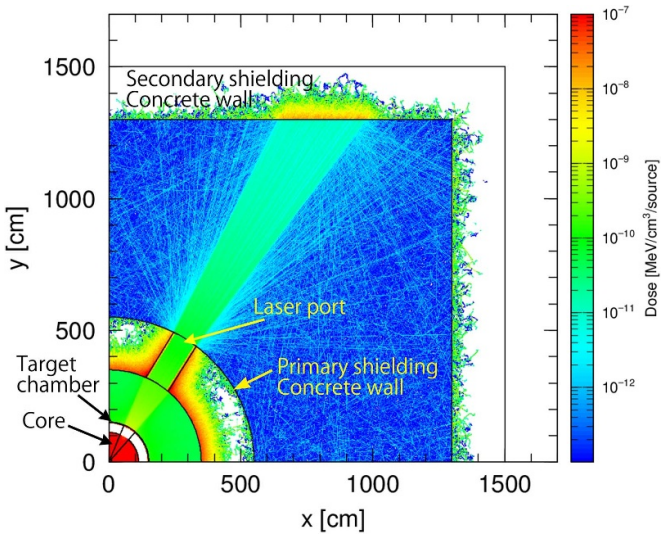

Figure 17. Energy deposited with the primary shield.

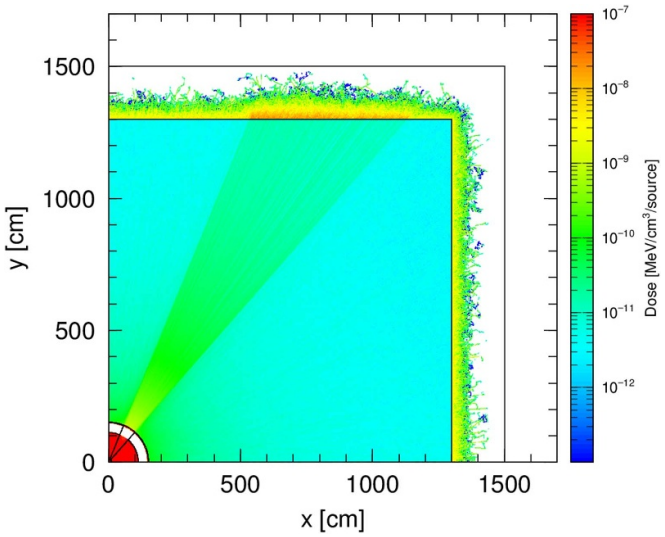

Figure 18. Energy deposited without the primary shield.

primary and secondary shield concept would provide full neutron shielding.

5. Development of target injection and tracking with L-Supreme

Target injection, tracking and engagement have been studied in each component, which might be applicable to future fusion reactors. However, to date, no system has demonstrated an integrated target injection, tracking and engagement system. Integration as a system is a remaining issue in order to realize fusion reactors. After commencing operation, L-Supreme would provide opportunities not only for plasma, blanket and material research, but also for the demonstration of integrated

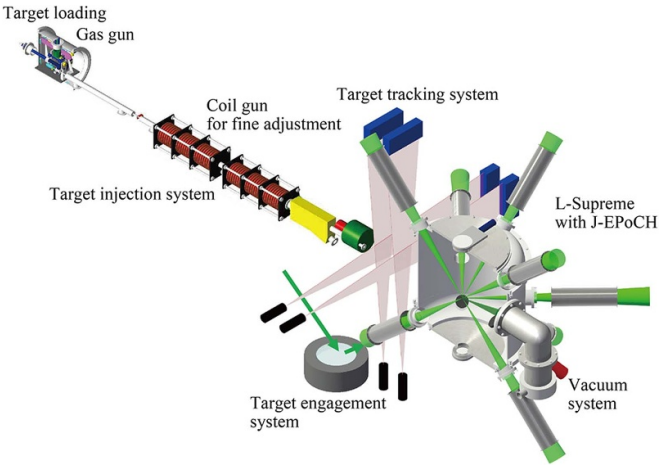

Figure 19. Conceptual drawing of an integrated demonstration system of target injection, tracking and engagement installed into L-Supreme.

target injection and tracking systems. Offsite development of target injection, tracking and engagement systems will be conducted in advance, according to the conceptual design of the Laser Inertial Fusion Test (LIFT) reactor [16]. Then, each system will be integrated into L-Supreme. Figure 19 shows the conceptual drawing of an integrated demonstration system of target injection, tracking and engagement. A target injection system consists of a gas gun for rough acceleration and coil gun for fine acceleration. Target velocity is adjusted at 100 ± 1 m s^{-1}. Then a target tracking system detects an injected target's trajectory. A candidate principle was discussed in [26]. A target engagement system predicts the target projected location at the chamber center and controls final optics. Proof of principle of a target engagement system has been demonstrated at University of California—San Diego [25]. The principle may be applicable to L-Supreme.

6. Summary

The feasibility of L-Supreme as a laser fusion research reactor system was assessed, considering existing technologies. According to the baseline design of L-Supreme, each system: the cores, target chamber, target delivery system, and EDS, can be produced without technology leaps. L-Supreme would be realized by putting the systems together.

Neutron shielding was briefly considered, in order to secure the safety of L-Supreme. The primary and secondary shield concept would provide a full neutron guard. The primary shielding is effective in reducing the energy deposited in the experimental hall. The concrete wall, 2 m thick, prevents neutrons from reaching the surrounding area of the experimental hall.

Table 2 summarizes the baseline design of L-Supreme.

Table 2. Summary of the baseline design.

Reactor type		Research reactor
Core		Replaceable for research
Laser system		J-EPoCH
	Energy	10 kJ class laser
	Beam number	Omnidirectional 12 laser beams
	Repetition	100 Hz of a maximum rate
Target		
	Type	LHART (Glass balloon containing gaseous DT at several 100 kPa)
	Size	1 mm diameter
Experimental condition		
	Batch	10 000 shots
	Target delivery rate	1 Hz
The amount of tritium		1.51×10^{8} Bq/LHART, 1.51×10^{12} Bq/batch
Neutron yield		10^{13} n/shot, 10^{17} n/batch
Fusion power (neutrons)		22.4 J/shot, 0.224 MJ/batch
EDS		
	1. Normal operation by once-through processes	
	Target chamber	>0.1 m^3 s^{-1} after a batch experiment >100 Nm^3 h^{-1} for a chamber purge
	Experimental hall	>3400 Nm^3 h^{-1} for a purge (tentative)
	Tritium lab.	>400 Nm^3 h^{-1} (tentative)
	EDS room	>500 Nm^3 h^{-1} (tentative)
	2. Emergency operation by internal circulation processes Circulation mode	
	Experimental hall	>4100 Nm^3 h^{-1} (less than 5000 Bq m^{-3} within 48 h)
	Tritium lab.	>500 Nm^3 h^{-1} (less than 5000 Bq m^{-3} within 12 h)
	EDS room	>1200 Nm^3 h^{-1} (less than 5000 Bq m^{-3} within 12 h)
Neutron shielding		
	Primary and secondary shielding concept	
	Primary shielding	2 m concrete wall with penetrations
	Secondary shielding	2 m concrete wall Full neutron shielding is provided

Acknowledgments

This work was performed with the support and under the auspices of the NIFS Collaboration Research Program (NIFS21KUGK139) and IFE forum, Japan.

ORCID iDs

Masahiro Tanaka https://orcid.org/0000-0001-9941-1958
Keisuke Shigemori https://orcid.org/0000-0002-3978-8427

References

[1] Bigot B. 2019 ITER construction and manufacturing progress toward first plasma *Fusion Eng. Des.* **146** 124–9
[2] Zylstra A.B. *et al* 2022 Burning plasma achieved in inertial fusion *Nature* **601** 542–8
[3] Kramer D. 2023 National Ignition Facility earns its name for a second time *Physics Today* (https://doi.org/10.1063/PT.6.2.20230811a)
[4] Kawamura Y. *et al* 2020 Progress of water cooled ceramic breeder test blanket module system *Fusion Eng. Des.* **161** 112050
[5] Basic Research Needs Workshop on Inertial Fusion Energy 2023 Report of the fusion energy sciences workshop on inertial fusion energy (U. S. Department of Energy)
[6] Goto T., Tanaka T., Tamura H., Miyazawa J., Iwamoto A., Yanagi N., Fujita T., Kodama R. and Mori Y. 2021 Feasibility study of tokamak, helical and laser reactors as affordable fusion volumetric neutron sources *Nucl. Fusion* **61** 126047
[7] Tobita K., Nishio S., Konishi S., Sato M., Tanabe T., Masaki K. and Miya N. 2003 First wall issues related with energetic particle deposition in a tokamak fusion power reactor *Fusion Eng. Des.* **65** 561–8
[8] Norimatsu T., Kawanaka J., Miyanaga M., Azechi H., Mima K., Furukawa H., Kozaki Y. and Tomabechi K. 2007 Conceptual design of fast ignition power plant KOYO-F driven by cooled Yb:YAG ceramic laser *Fusion Sci. Technol.* **52** 893–900
[9] Enoeda M. *et al* 2003 Design and technology development of solid breeder blanket cooled by supercritical water in Japan *Nucl. Fusion* **43** 1937–844
[10] Kondo M., Nakajima Y., Tanaka T. and Norimatsu T. 2018 Effect of isotope enrichment on performance of lead-lithium blanket of inertial fusion reactor *J. Phys.: Conf. Ser.* **1090** 012004
[11] Pereslavtsev P., Bachmann C. and Fischer U. 2016 Neutronic analyses of design issues affecting the tritium breeding performance in different DEMO blanket concepts *Fusion Eng. Des.* **109–111** 1207–11
[12] Tobita K., Hiwatari R., Sakamoto Y., Someya Y., Asakura N., Utoh H., Miyoshi Y., Tokunaga S., Homma Y. and Kakudate S. 2019 Japan's efforts to develop the concept of

JA DEMO during the past decade *Fusion Sci. Technol.* **75** 372–83
[13] Federici G. *et al* 2019 Overview of the DEMO staged design approach in Europe *Nucl. Fusion* **59** 066013
[14] Kitagawa Y., Sunahara A and Sentoku Y 2013 Hi-rep. counter-illumination fast ignition scheme fusion *Plasma Fusion Res.* **8** 3404047
[15] Nuttall W.J., Takeda S., Konishi S. and Webbe-Wood D. 2020 *Commercializing Fusion Energy: How Small Businesses are Transforming Big Science* (IOP Publishing)
[16] Norimatsu T., Kozaki Y., Shiraga H., Fujita H. and Okano K. 2017 Conceptual design and issues of the laser inertial fusion test (LIFT) reactor—targets and chamber systems *Nucl. Fusion* **57** 116040
[17] Ogino J. *et al* 2022 10-J, 100-Hz conduction-cooled active-mirror laser *Opt. Contin.* **1** 1270–7
[18] Sekine T. *et al* 2022 253 J at 0.2 Hz, LD pumped cryogenic helium gas cooled Yb:YAG ceramics laser *Opt. Express* **30** 44385–94
[19] Goodin D.T. *et al* 2004 A cost-effective target supply for inertial fusion energy *Nucl. Fusion* **44** S254–65
[20] Sakae S., Hayashi H., Kitabatake T., Matsumura T., Endo T. and Norimatsu T. 2009 Experiments on a gas gun for target injection in inertial fusion energy *Plasma Fusion Res. Rapid Commun.* **4** S1006
[21] Koga M., Uchino S., Maeda E., Yamanoi K. and Iwamoto A. 2022 Behavior of gas injected fast ignition targets *Plasma Fusion Res.* **17** 2404052
[22] Komeda O. *et al* 2013 First demonstration of laser engagement of 1 Hz injected flying pellets and neutron generation *Sci. Rep.* **3** 2561
[23] Mori Y. *et al* 2022 Ten hertz bead pellet injection and laser engagement *Nucl. Fusion* **62** 036028
[24] Carlson L.C., Tillack M.S., Stromsoe J., Alexander N.B., Flint G.W., Goodin D.T. and Petzoldt R.W. 2010 Completing the viability demonstration of direct-drive IFE target engagement and assessing scalability to a full-scale power plant *IEEE Trans. Plasma Sci.* **38** 300–5
[25] Carlson L., Tillack M., Stromsoe J., Alexander N., Goodin D. and Petzoldt R. 2009 Improving the accuracy of a target engagement demonstration *Fusion Sci. Technol.* **56** 409–16
[26] Tsuji R., Endo T., Yoshida H. and Norimatsu T. 2016 Development of position measurement unit for flying inertial fusion energy target *J. Phys.: Conf. Ser.* **688** 012124
[27] Goodin D.T. *et al* 2006 Developing a commercial production process for 500 000 targets per day: a key challenge for inertial fusion energy *Phys. Plasmas* **13** 056305
[28] Iwamoto A., Fujimura T., Nakai M., Norimatsu T., Sakagami H. Shiraga H and Azechi H 2013 FIREX foam cryogenic target development: residual void reduction and estimation with solid hydrogen refractive index measurements *Nucl. Fusion* **53** 083009
[29] Nagai K. *et al* 2005 Foam materials for cryogenic targets of fast ignition realization experiment (FIREX) *Nucl. Fusion* **45** 1277–83
[30] Iwamoto A. and Kodama R. 2020 Conceptual design of a subcritical research reactor for inertial fusion energy with the J-EPoCH facility *High Energy Density Phys.* **36** 100842
[31] Iwamoto A. and Kodama R. 2021 Core size effects of laser fusion subcritical research reactor for fusion engineering research *Nucl. Fusion* **61** 116075
[32] Takabe H. *et al* 1998 Scalings of implosion experiments for high neutron yield *Phys. Fluids* **31** 2884–93
[33] Norimatsu T., Tajima H., Takagi M., Nakai S. and Yamanaka C. 1988 Fabrication of large-diameter, high-aspect-ratio glass microballoon targets for laser fusion research *J. Vac. Sci. Technol.* A **6** 2552–5
[34] Sato T. *et al* 2024 Recent improvements of the particle and heavy ion transport code system—PHITS version 3.33 *J. Nucl. Sci. Technol.* **61** 127–35
[35] Fischer U., Bachmann C., Palermo I., Pereslavtsev P. and Villari R. 2015 Neutronics requirements for a DEMO fusion power plant *Fusion Eng. Des.* **98–99** 2134–7
[36] Moro F., Del Nevo A., Flammini D., Martellli E., Mozzillo R., Noce S. and Villari R. 2018 Neutronic analyses in support of the WCLL DEMO design development *Fusion Eng. Des.* **136** 1260–4
[37] Aoyama Y., Hasegawa Y., Sasaki M., Nakatsugawa J., Iwaji Y. and Komura A. 2018 Development of high-acceleration linear motor to realize resource saving and high productivity *Electr. Eng. Japan* **202** 55–63
[38] Wavrik R., Boyes J., Olson C., Dempsey F., Gracia R., Karpenko V., Anderson A., Tobin M. and Latkowski J. 1994 Target area chamber system design for the National Ignition Facility *Fusion Technol.* **26** 785–90
[39] Japan Industrial Standard (JIS) B8267 2020 *Construction of Pressure Vessel* (Tokyo Japanese Standards Association)
[40] ANEST IWATA Corporation 2009 Instruction manual of ISP-1000 (ANEST IWATA Corporation)
[41] Saito K., Sato Y., Inayoshi S. and Tsukuhara S. 1996 Measurement system for low outgassing materials by switching between two pumping paths *Vacuum* **47** 749–52
[42] Tanaka M., Kato H., Suzuki N., Masuzaki S., Yajima M., Nakada M. and Iwata C. 2020 Tritium balance in large helical device during and after the first deuterium plasma experiment campaign *Plasma Fusion Res.* **15** 1405062
[43] Tanaka M., Iwata C., Nakada M., Kato A. and Akada N. 2022 Levels of atmospheric tritium in the site of fusion test facility *Radiat. Prot. Dosim.* **198** 1084–9
[44] Tanaka M., Suzuki S., Kato H., Kondo T., Yokosawa M., Kawamuta T., Ikeda M., Meguro T., Tanaka T. and Sonoi K. 2018 Design and commissioning of the exhaust detritiation system for the Large Helical Device *Fusion Eng. Des.* **127** 275–83
[45] Tanaka M., Suzuki N., Kato H. and Chimura H. 2021 Performance of exhaust detritiation system for a fusion test device in the initial phase of the operation *Fusion Eng. Des.* **164** 112172
[46] Wilson J., Becnel J., Demange D. and Rogers B. 2019 The ITER tokamak exhaust processing system design and substantiation *Fusion Sci. Technol.* **75** 794–801
[47] Kohut T.R., Brereton S.J. and Khater H. 2013 Radiological design aspects of the National Ignition Facility *Health Phys.* **104** 557–62
[48] Research Committee on Shielding Handbook 2015 *A Handbook of Radiation Shielding—Basics* (Atomic Energy Society of Japan) pp 350–1